Scientific Research

Numerical Study on Cross-Frame Detailing Methods for Curved-Girder Bridges

Yuhao Li [1], Haiying Ma [1], Chivorn Sao [1], Bin Yan [2,*], Qiang Liu [3] and Komarizadehasl Seyedmilad [4]

[1] Dept. of Bridge Engineering, School of Civil Engineering, Tongji University, Shanghai,200092, China;
[2] College of Civil and Transportation Engineering, Beijing University of Technology, Beijing, 100124, China;
[3] Beijing Construction Engineering Group Co., Ltd., Beijing, 100044, China;
[4] Dept. of Civil and Environment Engineering, Universitat Politècnica de Catalunya (UPC), BarcelonaTech. C/Jordi Girona 1-3,Barcelona, Spain, Barcelona, 08034, Spain.
* Correspondence: yanbin@bjut.edu.cn

Abstract: Curved-girder bridge systems, owing to the bending–torsion coupling effect, tend to rotate out of plane under vertical loading. Compared with straight girder bridges, curved-girder bridges face greater difficulties during construction, particularly in regard to cross-frame installation. Three types of cross-frame detailing methods are employed, where the cross-section achieves the desired fit on the basis of the load type: no load fit (NLF), steel dead load fit (SDLF), and total dead load fit (TDLF). One of these methods determines the bridge's final shape and workability; thus, in this study, curved multiple-girder bridges with different curvatures are studied numerically to examine the effects of different cross-frame detailing methods on the internal forces, deformations, and load-bearing capacities of curved-girder bridges. This study focuses on the construction stage, so only the steel dead load and weight of the concrete slab are considered. The analysis results reveal that for bridges with small curvature radii, the use of an SDLF or a TDLF reduces bridge deformation (vertical deflection and rotation) but increases internal forces relative to the NLF. When the curvature radius increases, the influence of the SDLF and TDLF on the bridge's response diminishes. The study findings can be helpful for choosing proper detailing methods to use in the construction of composite curved I-girder bridges with various curvature radii.

Keywords: cross-frame; composite I-girder; curved-girder bridge; numerical analysis; bridge construction

Citation: Li, Y.; Ma, H.; Sao, C.; Yan, B.; Liu Q.; Komarizadehasl, S. Numerical Study on Cross-Frame Detailing Methods for Curved-Girder Bridges. *Prestress Technology* **2025**, *4*, 25-39. https://doi.org/10.59238/j.pt.2025.04.003

Received: 09/09/2025
Accepted: 26/11/2025
Published: 25/12/2025

1 Introduction

Curved-girder bridges are important in the construction of urban traffic and expressways in mountainous areas because bridge shapes are flexible. One advantage is that they satisfy the demanding requirements of mountainous expressways and improve traffic flow in the approach sections of significant bridges, junctions with major metropolitan routes, etc. Composite curved-girder bridges have more complex characteristics than straight girder bridges do and require more complicated erection processes because of the curvature. Even without a load acting on it, the curved I-girder significantly exhibits bending and torsional deformations because of the bending–torsion coupling effect. Under vertical loading, these effects are greatly magnified, leading to further bending–torsion deformation [1,2]. In curved I-girder bridge construction, cross-frames are essential for controlling cross-sectional deformations, thereby improving the overall structural geometry. To achieve this, the fitting of cross-frames must be carried out correctly before the erection process. The final outcome directly affects the bridge's overall response and constructability. Because individual girders possess low torsional stiffness and strength, they are prone to deformation and stress under their own weight. In addition, temporary support is necessary during the installation of cross-frames in

curved-girder bridges [3]. The impact of the temporary shoring location during construction on girder deformation is also significant, and the effects vary depending on the bridge curvature radii and erection sequences [4].

Generally, the detailing methods are designed to connect cross-frames to girders to reach fit conditions (Figure 1), including (1) NLF: the cross-frames are detailed to fit to the girders in the undeformed geometry under the no-load state; (2) SDLF: the cross-frames are detailed to fit to the girders, which are assumed to be nearly plumb under the self-weight of the girders and cross-frames (steel dead load) before the concrete deck is cast; and (3) TDLF: The cross-frames are detailed to fit to the girders in the plumb position under the no-load state, in which the girders are assumed to be nearly plumb under the total dead loads [5].

a) No Load Fit (NLF) b) Steel Dead Load Fit (SDLF) c) Total Dead Load Fit (TDLF)

Figure 1 Fit conditions based on the geometry under the total dead load

There are several challenges associated with the construction of curved bridges, including the stresses being relatively low during the erection phase, progressively increasing as the cross-frames are put into place, and becoming even more intensified after the deck placement [6]. In a study conducted in 2005, inconsistency in detailing subsequently caused the cross-frame members to misfit with the intended webs, resulting in difficulty and delay in construction. If forcibly erected, the unaccounted stress of each member will develop [7]. Furthermore, web out-of-plumb during construction was shown to influence bridge flange tip stresses, increase vertical and lateral deflections, and heighten the sensitivity of cross-frames [8]. These factors significantly complicate the construction process and directly impact the final shape of the bridge. Moreover, they could make the bridge unusable once construction is complete; thus, all these issues must be considered before construction. To address this, tools have been proposed to simplify cross-frame fitting in curved bridges, such as systems that use cables and hydraulic jacks to adjust girder geometry without relying on force fitting in highly curved bridges [9]. Nevertheless, selecting an appropriate cross-frame detailing method for a given bridge curvature remains critical to ensure controllability and a predictable structural response during construction.

Numerous experimental and numerical studies have investigated the behavior of composite curved bridges and their cross-frames. For example, one experiment investigated the mechanical properties of a twin I-girder bridge and highlighted the importance of cross-frames in resisting web distortion and transmitting torsional moments, albeit at the cost of increasing lateral bending moments in the bottom flanges [10]. The response of different cross-frame types in actual bridges under controlled vehicle loads has also been studied [11]. Several approaches have been used to study slender curved and skewed I-girder bridges. For instance, one analytical study addressed the challenges associated with concrete deck placement and validated its results against experimental data [12]. Other studies have examined full-scale curved bridges with various erection types under different conditions using analytical tools calibrated with experimental data to predict erection-stage responses [13]. In 2005, a simplified single-curved I-girder numerical model was proposed as an alternative to complex bridge systems. While such models accurately capture plasticity spread, flexural strength, and failure mechanisms, they are less

 https://doi.org/10.59238/j.pt.2025.04.003

effective in predicting the elastic stiffness and deflections of steel bridge girders [14]. Several numerical studies on curved steel I-girder bridges have also been conducted [15-17]. Notably, [15] thoroughly investigated various modeling strategies for analyzing the qualities and limitations of composite curved steel I-girder bridges. In summary, these studies reiterate the importance of cross-frames in curved I-girder bridges during both construction and service. However, the specific effects of different cross-frame detailing methods have not been directly addressed.

The primary objective of enhancing the behavior of curved-girder bridges is to increase their torsional stiffness and strength. In 2010, a proposal was made to improve the performance of bridges by using curved steel I-girders with steel tubes as flanges (tubular flange girders, or TFGs). These girders offer higher torsional stiffness and strength than regular steel I-girders do [18, 19]. Additionally, numerical and experimental research has shown that a different type of girder, similar to the previous proposal but with a simplified girder cross-section that uses only one steel tube in the top flange and steel plate in the bottom flange (TFG1), outperforms conventional steel I-girders in almost all aspects, most notably in that it does not require temporary support during construction [20].

To date, existing research and design specifications have not adequately addressed the effects of different cross-frame detailing methods on bridge responses across varying curvature radii, including internal forces and deformations. Proper understanding of these effects can provide more insight into how to correctly choose which method is suitable for cross-frame detailing.

This paper presents a numerical study using finite element simulation to simulate and analyze the installation processes of cross-frames using three different detailing methods (NLF, SDLF, and TDLF) on different curvature radii of composite curved-girder bridges. This research aims to investigate the responses of bridges under different cross-frame detailing methods and to identify which types are most effective for various bridge curvature radii.

2 Cross-Frame Detailing Methods

"Fit" refers to a state of girders, deflected or undeflected geometry, influencing how cross-frames are detailed to attach to girders in the theoretical plumb or no-load state. It is imperative to understand the concept of the no-load state since each girder must be in the no-load state before being connected with a cross-frame. A no-load state girder essentially refers to a girder being supported with several temporary shoring structures or supports. Thus, the girders can be assumed to be erected in the no-load state. Temporary shoring or supports can help girders achieve this state by effectively curbing displacement and rotation. Cross-frames are originally installed on the girders in the no-load state. Thus, if even one girder is not in the intended geometry, owing to the bending–torsion coupling effect, the construction will be problematic and affect the bridge's final shape [21]. Below are the procedures for installing cross-frames for each detailing method [22].

2.1 No Load Fit (NLF)

Each girder is fabricated with a camber, and cross-frames are immediately connected to both girders in the no-load state by employing temporary supports. As shown in Figure 2a), prior to connection, the difference in elevation between the two vertically plumb and fully cambered girders is Δ_0, and the vertical distances between the girders and the desired elevation are Δ_1 and Δ_2, respectively. After the cross-frames are connected to the girders, the temporary supports are removed, and the additional weight of the concrete slab is applied. The final state of the bridge's cross-sectional geometry is shown in Figure 1a).

2.2 *Steel Dead Load Fit (SDLF)*

To install cross-frames using the SDLF, external forces, specifically torsion, are applied to the girder during the construction process to offset the difference in elevation between one girder and another girder with cross-frames installed. The process of installing cross-frames using the SDLF is shown in Figure 2. (1) Prior to connection, the difference in elevation between the vertically aligned and fully cambered girders is Δ_0, and the vertical distances between the girders and the desired elevation are Δ_1 and Δ_2, which are the same as those when the NLF method is used (see Figure 2a)). (2) When one end of the cross-frame is attached to Girder A, the difference in elevation between the two girders becomes Δ_s (see Figure 2b)). (3) When an external force M_s' is exerted on the girder with the cross-frame attached, the other end of the cross-frame is connected to Girder B. The applied external force M_s' is equal to the torque generated by the combined weight of the cross-frame and girders but in the opposite direction (see Figure 2c)). (4) The temporary supports are removed so that the only forces acting on the girders are the self-weights of the girders and cross-frame (see Figure 2d)). (5) The concrete deck is then placed. This step is visualized in Figure 2e). By applying an external force equal to the weight of the steel components to fit the girder with the cross-frame, the SDLF method results in an approximately plumb position for the bridge's cross-section when the temporary supports are removed and the only acting forces are the self-weight of the girder and the cross-frame (Figure 2d)).

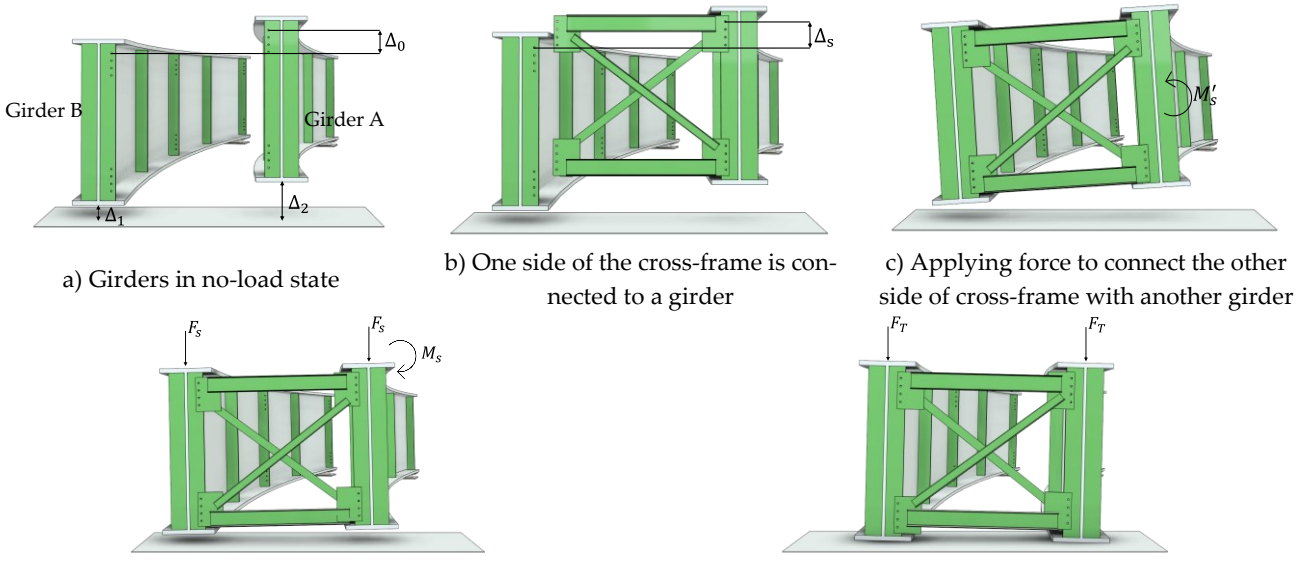

a) Girders in no-load state

b) One side of the cross-frame is connected to a girder

c) Applying force to connect the other side of cross-frame with another girder

d) Steel dead load acting on the structure

e) Total dead load acting on the structure

Figure 2 The installation process of cross-frames (SDLF)

2.3 *Total Dead Load Fit (TDLF)*

To achieve the desired geometry of the cross-section using the TDLF method, it is necessary to provide an appropriate external force (torsion) during the erection of cross frames, similar to the approach used in the SDLF method. This force counteracts the torsional deformation of the cross-section caused by the total dead load, making the required applied force larger than that in the SDLF method. The magnitude is equal to the torque generated by the total weight of the structure, including the concrete deck. Thus, the TDLF method results in an approximate plumb position under the total dead load (Figure 1c)).

2.4 *Comparisons of the Detailing Methods*

The NLF method, a typical cross-frame erection technique, involves installing cross-frames in a no-load state. In contrast, the SDLF and TDLF methods require

https://doi.org/10.59238/j.pt.2025.04.003

external forces to connect cross-frames to the girders. For the SDLF, the self-weight of the steel components (girders and cross-frames) causes the girders to rotate back to their deflected plumb positions before the concrete is cast. In the TDLF, the total dead load—including both the self-weight of the steel and the concrete deck—induces this counterrotation, causing the cross-section to approximately plumb under the total dead load. Although the SDLF and TDLF share the same erection processes, the two differ from the NLF because external forces are applied to eliminate initial elevation differences between cross-frames and girders, and the cross-frames do not fit the girders in the initial no-load state.

3 Finite Element Modeling

3.1 Example Bridge

The bridge used in this study is based on an expressway ramp bridge along the Yangtze River in Sichuan Province, which is a composite curved girder bridge with a span of 5×50 m and a radius of curvature of 200 m. A parametric analysis is conducted on the basis of this bridge design (Figure 3). The bridge models consist of five continuous spans, with four girders arranged from G1 (innermost girder, closest to the center of curvature) to G4 (outermost girder). The bridge spans are numbered as shown in Figure 4a). Five bridge types with different radii were chosen, ranging from 100 m, 200 m, 300 m, 400 m to 500 m.

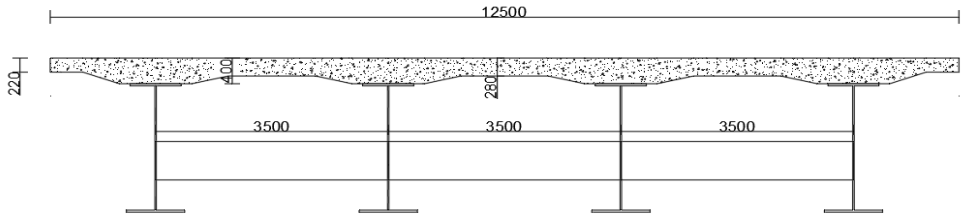

Figure 3 Standard bridge cross-section (unit: mm)

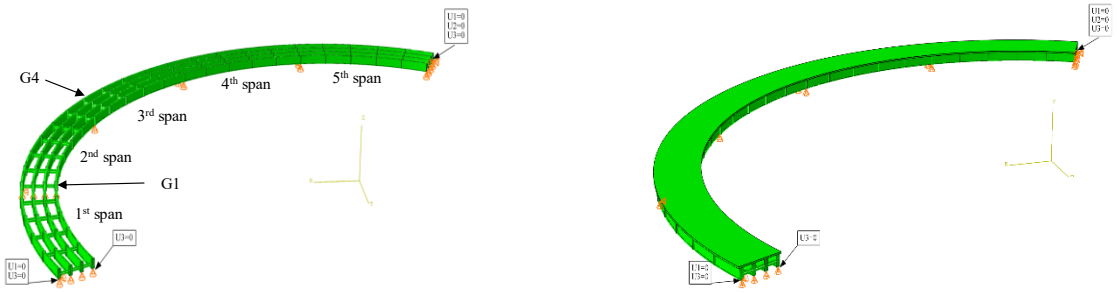

a) Without concrete deck b) With concrete deck

Figure 4 Basic bridge finite element models

3.2 Element Types and Boundary Condition Characteristics

The finite element (FE) model of the horizontally composite curved girder bridge system, established using the same modeling procedure, was experimentally validated [23]. The results show that the FE model is in good agreement with the experimental results and can accurately predict structural performance. Thus, FE modeling methods are adopted in this paper.

Finite element models were developed in ABAQUS 2020 to simulate cross-frame installation. By accurately defining boundary conditions and element connections, the installation process is repeated step by step to evaluate the effects of cross-frame detailing methods on the internal forces and deformations of completed bridges.

The webs and the stiffeners are all modeled using linear quadrilateral shell elements (S4R). Girder flanges and cross-frames are modeled using rectangular beam elements and I-shaped beam elements, respectively, with the same B31 type.

Multipoint constraints (MPCs) are used to connect nodes between different components, as shown in Table 1.

Table 1 Multipoint constraints (MPCs) for each connection type

Connection		MPC type
Set A	Set B	
Flanges	Webs	MPC (Beam)
Flanges	Stiffeners	MPC (Beam)
Webs	Stiffeners	MPC (Tie)
Stiffeners	Cross-frames	MPC (Beam)
Top flanges	Concrete deck	MPC (Beam)

The concrete bridge deck is modeled using solid elements with an elastic modulus of 34.5 GPa, Poisson ratio of 0.2, and a coefficient of thermal expansion of 0.00001. For the flanges, webs, and cross-frames, the elastic modulus of the steel material is 206 GPa, the Poisson's ratio is 0.31, and the coefficient of thermal expansion is 0.000012.

As displayed in Figure 4, the boundary conditions of the final structures are constrained at the support position for the bottom flange nodes of each girder in the vertical direction (U3=0), except that the exterior girder G4 is constrained both vertically and radially (U3=0, U1=0), and the nodes at the bottom flange at span 5 of G4 are constrained in the circumferential direction (U2=0).

3.3 Finite Element Modeling Process

This section introduces the finite element simulation process for the SDLF method. As shown in Figure 5, the finite element simulation process can be divided into 5 steps: a) simulate the no-load state of the structure: place the temporary supports, apply full constraints to the bottom flange nodes of each girder (U1=U2=U3=0), and apply radial constraints to the web nodes of each main girder (U1=0); b) connect one end of the cross-frame to the girder, then combine the elements between the two to ensure displacement compatibility; c) apply the displacement load (Δ_s) to the node of another end of the cross-frame to simulate the pretorsion applied when installing the cross-frame; d) connect that end of the cross-frame to the girder; and e) remove the temporary support constraint, retaining only the permanent supports (Figure 4).

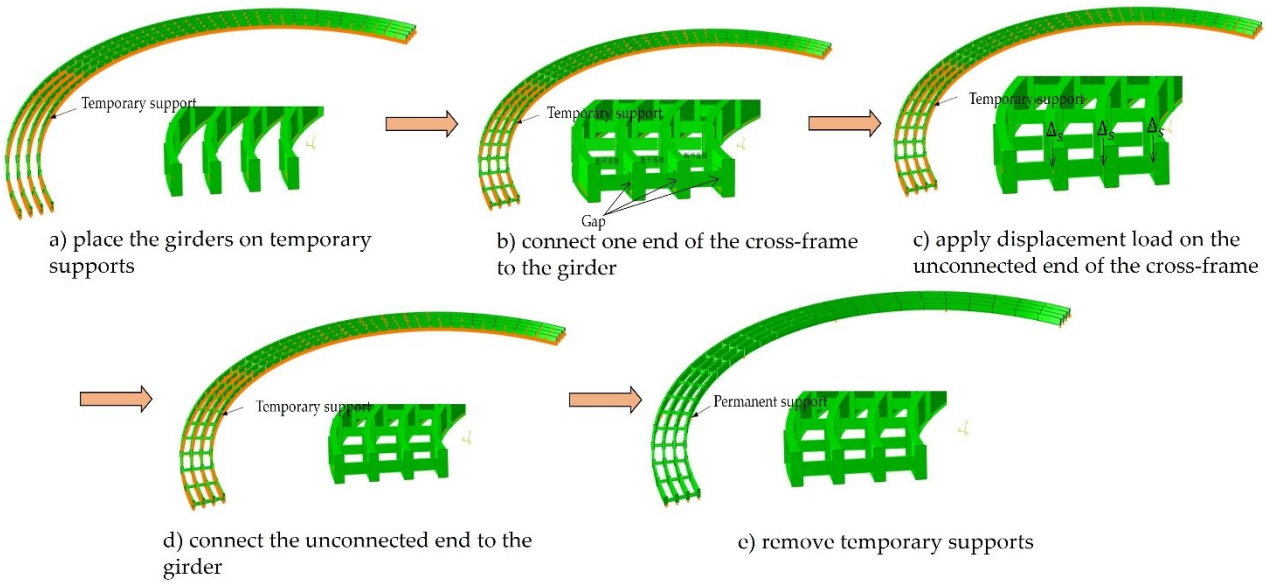

Figure 5 The modeling process of cross-frame installation

https://doi.org/10.59238/j.pt.2025.04.003

With respect to the NLF method, step (a) of the process remains unchanged; after this step, the cross-frame is connected directly to the girder without applying an external load, and the temporary support is removed immediately afterward. The magnitude of the displacement load (Δ_s) differs between the SDLF and TDLF and is calculated on the basis of the desired state of the bridge cross-section under the total dead load (specifically, the torque generated by the steel dead load for the SDLF and by the total dead load for the TDLF).

4 Results and Discussion

Analyses and comparisons of internal forces, torsion, and final elevations are conducted for the three different detailing methods.

4.1 Internal Forces Analysis

It is concluded that the critical girder G4 at mid-span sections of spans 1 and 5 has the greatest internal forces among all the girders in the bridge, and the results of G4 are selected to compare the effects of different detailing methods. Tables 2 and 3 summarize the internal forces at mid-span sections of spans 1 and 5 for the exterior girder (G4) across different bridge curvatures. The data in Table 2 indicate that the various detailing methods have pronounced effects on the bending moment, particularly for bridges with radii of 100 m and 200 m. In comparison, the effects on bridges with radii greater than 300 m are less pronounced. An increase in the bending moment at the upper flange of the girder and a decrease at the lower flange are observable for the SDLF and TDLF compared with the NLF. As shown in Table 3, compared with the NLF, the SDLF and TDLF reduce the torque at the top and bottom flanges of the girder.

Table 2 Bending moment M_T (kN·m) in the mid-span sections of spans 1 and 5 of G4

Curvature radius (m)	NLF		SDLF		TDLF	
	TF	BF	TF	BF	TF	BF
100	317	407	345	403	416	390
200	127	158	134	156	145	152
300	81	95	84	94	85	92
400	61	67	63	66	63	64
500	50	51	52	51	46	48

Note: TF and BF are the abbreviations for top flange and bottom flange, respectively.

Table 3 Torque M_R (kN·m) in the mid-span sections of spans 1 and 5 of G4

Curvature radius (m)	NLF		SDLF		TDLF	
	TF	BF	TF	BF	TF	BF
100	1.328	0.96	1.323	0.96	1.305	0.95
200	0.99	0.73	0.98	0.72	0.96	0.71
300	0.88	0.65	0.87	0.64	0.87	0.64
400	0.83	0.61	0.82	0.6	0.82	0.6
500	0.79	0.58	0.79	0.58	0.8	0.6

The SDLF and TDLF cross-frame installation methods increase the cross-sectional bending moment and torque of the girders in composite curved-girder bridges. This occurs because the cross-frames force the main girders to maintain a position closer to vertical, thereby resisting their torsional tendency. For bridges with a curvature radius of 100 m, compared with the NLF method, the bending moment of the top flange under the SDLF and TDLF increase by approximately 8.8% and 31.2%, respectively. When the curvature radius increases to 300 m, the bending moment increases by 16% under the SDLF and 4.3% under the TDLF. For a bridge with a 500 m curvature radius, the bending moment of the SDLF increases by up to 2%, whereas that of the TDLF decreases by approximately 8%. With respect to cross-

sectional torque, the influence of different cross-frame installation methods is relatively minor. The general trend shows that as the curvature radius increases, the torque values for the SDLF and TDLF decrease relative to those of the NLF.

4.2 Torsion Analysis

Curved girder bridges under total dead load generate bending moments and coupled torsion because of the influence of curvature. If cross-frames are not connected to the girders, a single girder alone will experience significant torsional deformation. The cross-frames provide torsional stiffness, transferring torque to adjacent girders and thus enhancing the overall rigidity of the structure. The results of the analysis reveal that G4 has the most significant torsion angle; therefore, its results are used to compare various detailing methods. As depicted in Figure 6, small and abrupt changes are exhibited in the torsion angles, specifically at points where the cross-frames connect. The abrupt changes arose because of cross-frames trying to rotate the girder back to its original position. The original position is where the cross-frames connect to the girders, without a concrete deck load. Consequently, the rotation induced by the cross-frames is opposite to the rotation tendency of the girders under the total dead load.

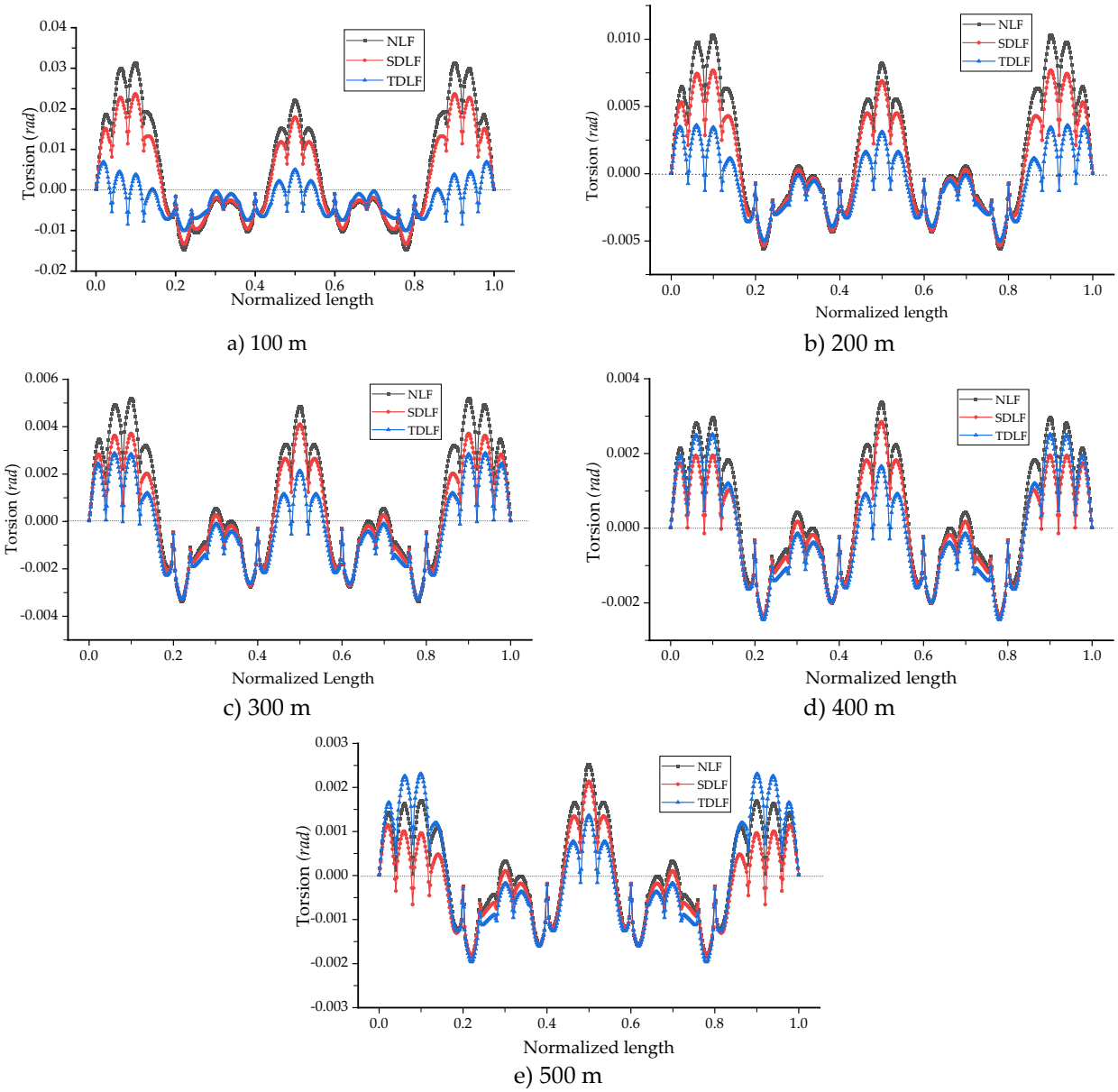

Figure 6 The influence of cross-frame installation methods on the cross-section torsion angle of composite curved bridges with different curvature radii under the action of total dead load

https://doi.org/10.59238/j.pt.2025.04.003

For the 5×50 m composite curved-girder bridges examined in this study, the cross-section reaches its maximum torsion angle at the mid-span sections of spans 1 and 5 (end spans) when the curvature radius varies between 100 m and 300 m. However, if the curvature radius exceeds 300 m, the largest torsion angle occurs in the mid-span section of span 3. The torsion direction of the cross-section at spans 2 and 4 is opposite to that at spans 1, 3, and 5, and their magnitudes are lower. For example, for a bridge with a radius of 100 m, the torsion angle of the NLF method is 0.0313 rad at spans 1 and 5 and 0.0221 at span 3. This trend remains consistent for all bridges with curvature radii of 300 m and below.

For curvature radii 300 m and below, the torsion angle of each span of the girder is arranged in the following order: NLF>SDLF>TDLF. With a curvature radius of 400 m, the torsion angles of spans 1 and 5 follow the sequence NLF>TDLF>SDLF, whereas the torsion angles of spans 2, 3, and 4 are arranged in the order NLF>SDLF>TDLF. When the radius is 500 m, the torsion angles in spans 1 and 5 follow the sequence TDLF>NLF>SDLF, whereas those in spans 2, 3, and 4 follow NLF>SDLF>TDLF. For composite curved-girder bridges with curvature radii exceeding 300 m, span 3 consistently has the greatest torsion angle. For instance, at a 400 m radius, the torsion angle of the mid span section of span 3 is 0.0033 rad when the NLF method is used, 0.0028 rad when the SDLF method is used, and 0.0016 rad when the TDLF method is used. The maximum torsion angle of the cross-section in span 3 across varying curvature radii generally follows the order of NLF>SDLF>TDLF.

In summary, when the curvature radius is less than 300 m, the structural response to dead load, specifically torsion, is highly sensitive to the cross-frame detailing method. The NLF, which involves no pretorsion to achieve fit conditions, fails to offset the torsional deformation induced by the total dead load. In contrast, the SDLF and TDLF use pretorsion to install cross-frames to the girder, resulting in the girders assuming a nearly plumb position under the total dead load. However, the constraining effects of the SDLF and TDLF on torsion in other spans (excluding span 3) demonstrate an inverse relationship with the curvature radius: as the radius increases, the constraint efficiency decreases. Consequently, the torsion angle tends to increase for the SDLF and TDLF relative to the NLF at larger radii.

As shown in Figure 7, the torsion angle at the mid-span sections of spans 1, 5, and 3 is inversely proportional to the curvature radius: as the radius decreases, the torsion angle increases. For a curvature radius of 100 m, the maximum torsion angle at spans 1 and 5 using the NLF method is 0.032 rad. At 300 m (same method), this angle decreases to 0.005 rad, and at 500 m, it does not exceed 0.002 rad. Bridges with curvature radii less than 200 m experience stronger effects, with the magnitude intensifying as the radius decreases. However, when the curvature radius exceeds 400 m, the impact of the detailing methods on the torsion angle becomes insignificant.

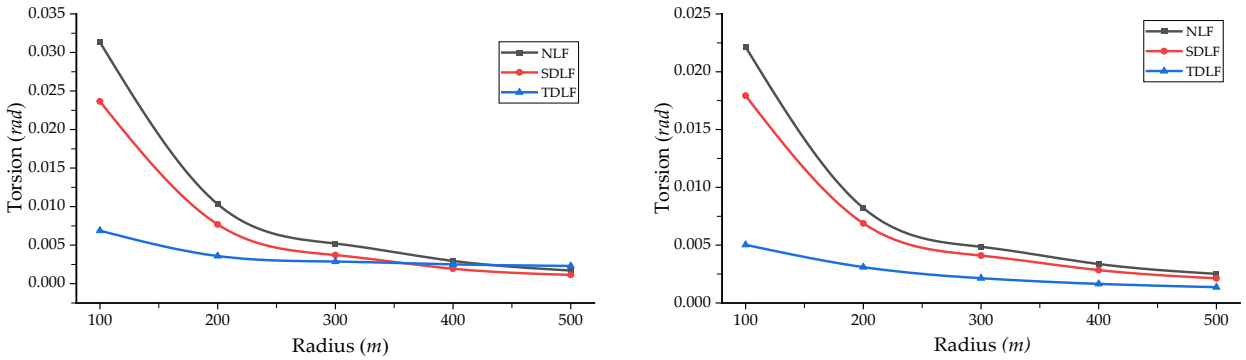

a) mid-span section of spans 1 and 5 b) mid-span section of span 3

Figure 7 The influence of cross-frame installation methods on the maximum torsion angle of composite curved bridges with different curvature radii

4.3 *Target Elevation*

The relative change in deflection is evaluated to assess the deviation between the actual elevation at completion and the target elevation of the girder. The vertical deflection induced by total dead load, calculated using the NLF method, indicates that girders achieve the target elevation. This establishes NLF as the benchmark for precise girder positioning at the specified elevation upon bridge completion. Consequently, vertical deflection disparities from other methods are compared against the NLF method, enabling a systematic comparison of detailing methods.

Taking G4 with the greatest deflection for comparison, as depicted in Figure 8, when the curvature radius ranges from 100 m to 200 m, the deviation between the actual and target bridge elevations follows the order TDLF > SDLF > NLF. Specifically, for spans 1, 3, and 5, TDLF and SDLF produce elevations higher than the target, whereas spans 2 and 4 show elevations lower than the target.

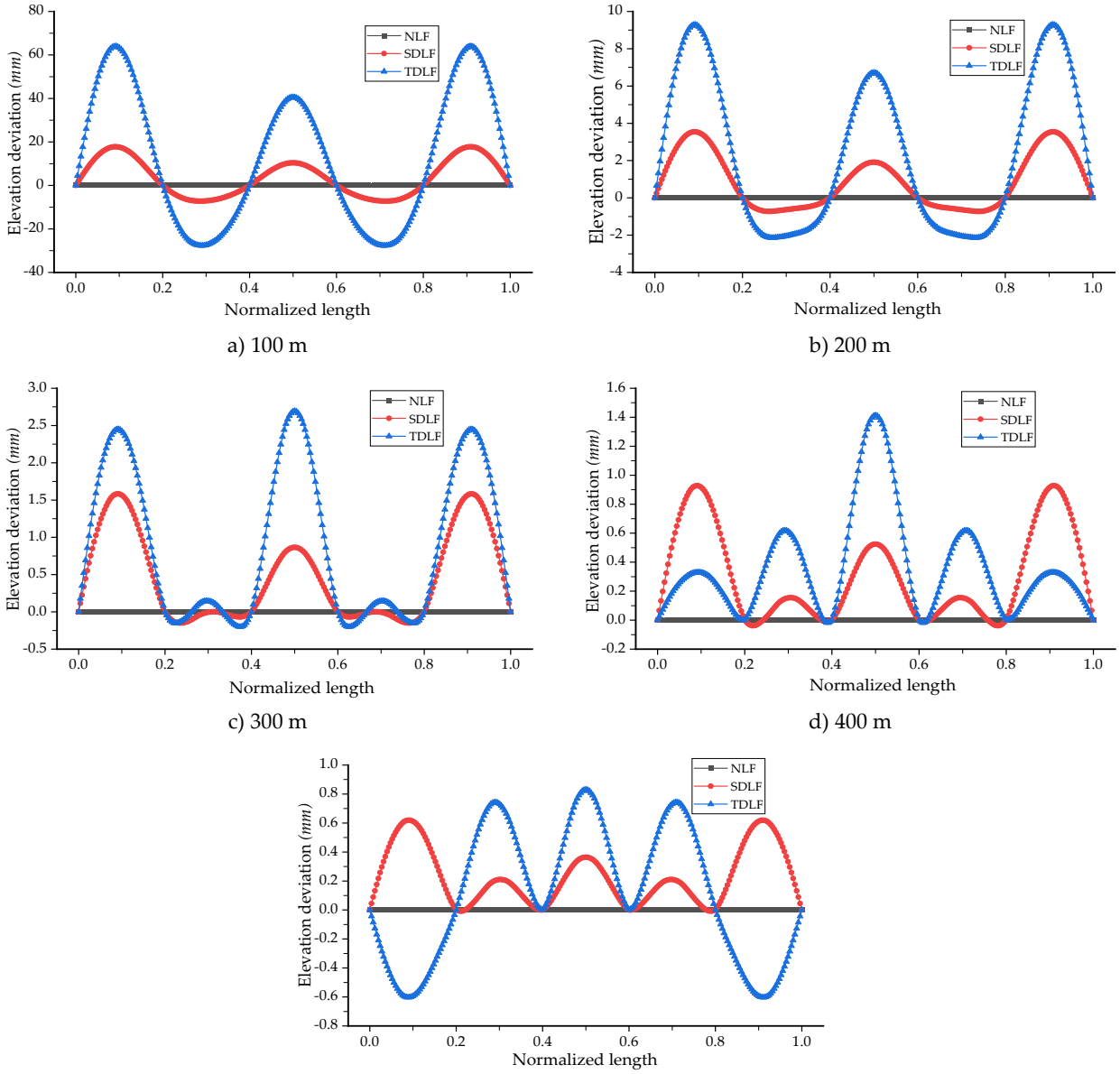

Figure 8 The influence of cross-frame installation methods on the final elevation of composite curved bridges with different curvature radii under the action of total dead load

The elevation deviation under total dead load fit (TDLF) reaches more than 60 mm for the bridge with a curvature radius of 100 m and 9.28 mm for the bridge with

https://doi.org/10.59238/j.pt.2025.04.003

a curvature radius of 200 m. This finding indicates that both TDLF and steel dead load fit (SDLF) result in significant deflection from the target elevation but minimal rotational (torsional) displacement. At curvature radii of 300 m or greater, the maximum elevation deviation for the TDLF and SDLF does not exceed 3 mm.

The correlation between the curvature radius and maximum deflection at the mid-span sections of spans 1, 5, and 3 is shown in Figure 9. A 100 m radius induces the greatest elevation deviation for the TDLF, with mid-spans of spans 1 and 5 deviating by approximately 65 mm from the target. In contrast, the SDLF causes mid-span deviations of approximately 19 mm. As the curvature radius increases, the impact of each detailing method on girder elevation deviation progressively decreases. These trends indicate that the SDLF and TDLF have minimal effects on the final bridge deflection at radii exceeding 200 m, making the NLF the preferred method.

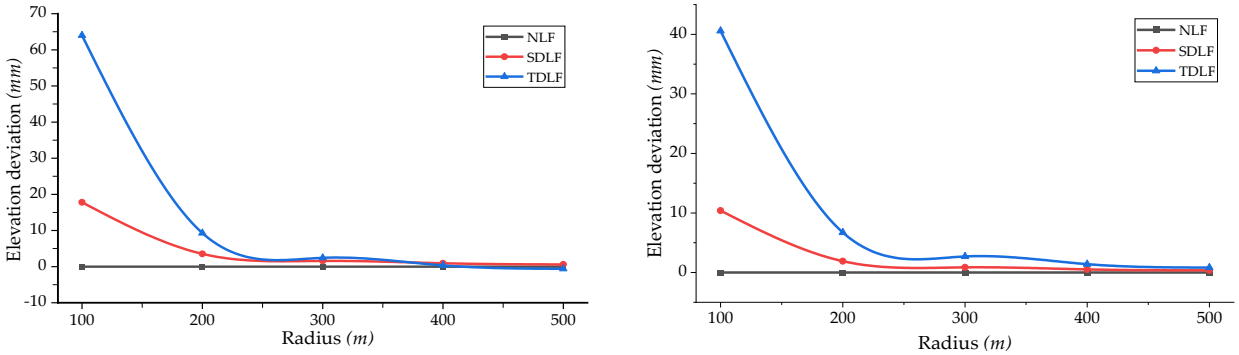

a) mid-span sections of spans 1 and 5 b) mid-span section of span 3

Figure 9 The influence of cross-frame installation methods on the elevation deviation of composite curved bridges with different curvature radii

The relationship between the torsion angle and vertical deflection is evident. For curved bridges with small curvature radii, the NLF method results in larger torsion angles, albeit the target elevation is reached.

4.4 Structural Bearing Capacity Analysis of Different Detailing Methods

The results from Sections 4.1 to 4.3 demonstrate that cross-frame detailing methods significantly influence internal forces and displacement in composite curved-girder bridges with small curvature radii. Accordingly, in this section, a composite curved-girder bridge model with a 5×50 m span and a 100 m radius of curvature is examined.

The analysis incrementally applies the bridge deck's distributed load to the structure, assessing the effects of three cross-frame detailing methods on the load-bearing capacity. Failure is defined as plastic hinge formation in the girder.

4.4.1 Analysis of Load-Bearing Capacity Using Nonlinear Considerations

(1) Geometrical nonlinearity

The load increment steps are determined during the analysis, with loads applied gradually to ensure that all load levels are imposed on the deforming structure. With NLGEOM enabled in ABAQUS's nonlinear geometric effects module, geometric nonlinearity is automatically computed throughout the analysis.

(2) Material nonlinearity

To ensure a conservative estimation of the structural bearing capacity, a bilinear constitutive model for Q345 steel was adopted. The yield stress is defined as the design strength value of 260 MPa for Q345 steel. The stress–strain curve of the steel constitutive model used in this study is shown in Figure 10.

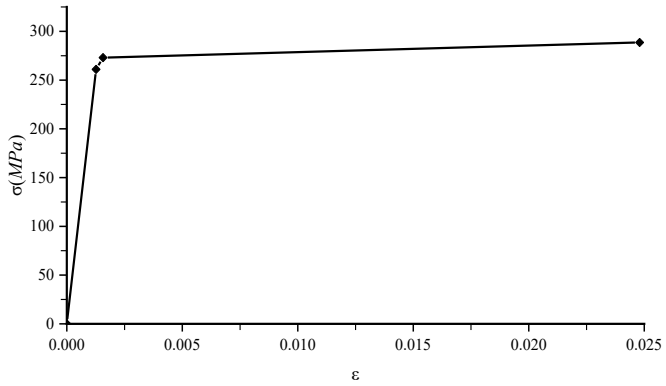

Figure 10 Q345 steel broken line constitutive model

Table 4 Constitutive model parameters for Q345 steel

No.	σ (MPa)	ε	Young's modulus (MPa)
1	0	0	
2	261	0.001267	205,998
3	273	0.00157	39,604
4	288.6	0.0248	671.5

4.4.2 Load-Bearing Capacity Analysis

The main steel structure is formed following the completion of the girder and cross-frame erection, but the casting of the concrete deck has not started. The weight of the bridge deck is considered an external load that is gradually applied to the bridge system, and the change in deflection is calculated to evaluate the structural load-bearing capability. On the basis of the load–displacement curve, the formation of a plastic hinge, indicating the girder's failure state, is defined by a decrease in the applied load alongside a continuing increase in vertical deflection.

Deflection at the mid-span section of span 1 is calculated for specified deck load levels. The results are depicted in Figure 11.

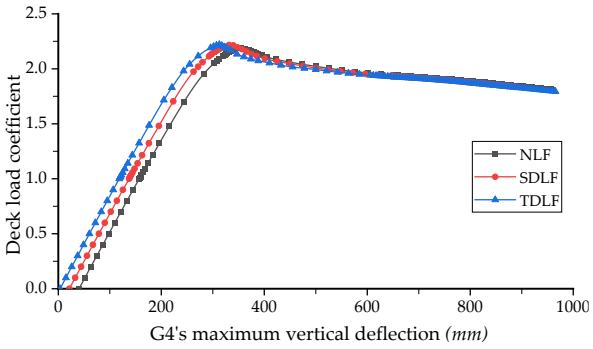

Figure 11 Comparison of deflection of G4 under different deck loads using different installation methods

When only the dead weight of the girders and cross-frames acts on the structure (prior to deck loading), the initial elevation of G4 varies significantly according to the detailing method: 40.2 mm (NLF), 21.4 mm (SDLF), and 3.4 mm (TDLF). The difference in initial elevation is influenced by whether the girder is pretorqued and the magnitude of pretorsion applied during cross-frame erection.

Under loading, the NLF method reaches its limit state at 2.19 times the bridge deck weight, with a deflection of 355.3 mm. At this point, local yielding occurs, preventing further load increase. Compared with the other methods, the SDLF and TDLF methods achieve higher capacities: 2.21 times (deflection: 331.7 mm) and 2.22 times (deflection: 314.6 mm) the deck weight, respectively. Post-yielding, the girder

 https://doi.org/10.59238/j.pt.2025.04.003

continues to deform despite load reduction—a characteristic behavior of plastic hinge formation.

In comparison to the NLF, the carrying capacity is increased by approximately 0.9% when the SDLF is used, and the deflection is 6.6% less than that when the NLF is loaded to the maximum capacity. With the TDLF, the carrying capacity is approximately 1.3% greater than that with the NLF, and the deflection is approximately 11.4% less than that with the NLF. SDLF and TDLF can reduce deflection when the girder reaches the maximum bearing capacity, but they have minimal effects on increasing the structure's bearing capacity.

5 Conclusions

In the present research, the finite element software ABAQUS is used to study the effects of different cross-frame detailing methods on bridges with curvature radii ranging from 100 m to 500 m. From the previous discussion, the following conclusions can be drawn:

(1) For bridges with small curvature radii of 100 m and 200 m, the detailing methods significantly influence the bending moments. Specifically, the bending moments of the top flanges increase and those of the bottom flanges decrease in the SDLF and TDLF methods, respectively. However, when the radius increases from 300 m, the influence becomes less noticeable. In contrast, the torques are lower for the SDLF and TDLF than for the NLF.

(2) For bridges with curvature radii of 100 m to 200 m, the SDLF and TDLF result in elevations that are higher than the desired elevation at spans 1, 3, and 5 and lower at spans 2 and 4. When the curvature increases, however, the difference between the actual and desired elevations remains below 3 mm.

(3) In bridges with curvature radii of 100 to 300 m, the maximum torsion angle occurs at the mid-span of spans 1 and 5. Variations in the torsion direction are observed across the spans, with span 3 exhibiting the largest torsion angles for bridges with curvature radii exceeding 300 m. In general, compared with the SDLF and TDLF, the NLF produces larger torsion angles. The TDLF minimizes the torsion angle and girder deflection in composite curved-girder bridges with curvature radii less than 100 m. For bridges with a curvature radius of approximately 200 m, the SDLF is sufficient to control torsional rotations, whereas the NLF is recommended for bridges with greater curvature radii.

(4) Although TDLF is effective at controlling girder deformations during construction, it may increase the flange stress (particularly in the upper flange) in bridges with small curvature radii. Therefore, the TDLF should be used with caution, as elevated stresses may complicate construction. If the SDLF is used instead, increasing the deck weight to bring the girders closer to the target elevation can be considered, since the torsional behavior of the SDLF is more comparable to that of the TDLF.

(5) Although cross-frame detailing methods are not effective at improving the bridge's bearing capacity, they do improve the bridge's deflections once it has reached its maximum bearing capacity.

(6) Further studies should focus on actual experiments to quantitatively evaluate the effects of each cross-frame detailing method on bridge responses throughout the step-by-step construction sequence.

Conflict of interest: All the authors disclosed no relevant relationships.

Data availability statement: The data that support the findings of this study are available from the corresponding author, Yan, upon reasonable request.

Funding: This research was funded by National Natural Science Foundation of China (52478318); Natural Science Foundation of Shanghai (24ZR1469500); Fundamental Research Funds of the Central Universities (2023-2-YB-17); Spanish Ministry of Science and Innovation (PID2021-126405OB-C31). The authors extended their sincere gratitude for the support.

References

1. Davidson, J.S. Stability research into the design of curved steel bridges. In *Analysis and Design of Plated Structures*, 2nd ed.; Shanmugam, N.E., Wang, C.M., Eds.; Woodhead Publishing: Cambridge, UK, **2022**; pp. 635–674, doi:10.1016/B978-0-12-823570-6.00010-0
2. Sennah, K.M.; Marzouck, M.H.; Kennedy, J.B. Horizontal bracing systems for curved steel I-girder bridges. In *Structural Engineering, Mechanics and Computation*; Zingoni, A., Ed.; Elsevier Science: Oxford, UK, **2001**; pp. 599–606, doi:10.1016/B978-008043948-8/50064-3
3. Stith, J.; Petruzzi, B.; Helwig, T.; Engelhardt, M.; Frank, K.; Williamson, E. Guidelines for design and safe handling of curved I-shaped steel girders. **2010**. https://rosap.ntl.bts.gov/view/dot/18284
4. Sharafbayani, M.; Linzell, D.G. Effect of temporary shoring location on horizontally curved steel I-girder bridges during construction. *J. Bridge Eng.* **2012**, *17*, 537–546, doi:10.1061/(ASCE)BE.1943-5592.0000269
5. Coletti, D.A.; White, D.W.; Nguyen, T.V.; Chavel, B.W.; Grubb, M.A.; Boring, C.G. Reliable fit-up of steel I-girder bridges. *Transp. Res. Rec.* **2017**, *2642*, 1–8, doi:10.3141/2642-01
6. Fasl, J.D.; Stith, J.C.; Helwig, T.A.; Schuh, A.; Farris, J.; Engelhardt, M.D.; Williamson, E.B.; Frank, K.H. Instrumentation of a horizontally curved steel I-girder bridge during construction. *J. Struct. Eng.* **2015**, *141*, 1–12, doi:10.1061/(ASCE)ST.1943-541X.0001110
7. Chavel, W.B.; Earls, C.J. Inconsistent detailing of cross-frame members in horizontally curved steel I-girder bridges. In *Structures Congress 2005*; ASCE: Reston, VA, USA, 2012; pp. 1–12, doi:10.1061/40753(171)34
8. Howell, T.D.; Earls, C.J. Curved steel I-girder bridge response during construction loading: Effects of web plumbness. *J. Bridge Eng.* **2007**, *12*, 485–493, doi:10.1061/(ASCE)1084-0702(2007)12:4(485)
9. Thrall, A.P.; Duarte, C.N.; Sun, S.Y.; Byers, D.D.; Zoli, T.P. Deployable tool to facilitate cross-frame installation in highly skewed and curved steel girder bridges. *J. Bridge Eng.* **2024**, *29(5)*: 04024015, doi:10.1061/JBENF2.BEENG-6160
10. Feng, B.W.; Liu, Y.J.; Yang, X.; Liu, J.; Zhang, G.J.; Ma, Y.P. Experimental research on curved continuous steel–concrete composite twin I-girder bridge. *Structures* **2023**, *54*, 669–683, doi:10.1016/j.istruc.2023.05.081
11. Reichenbach M C, White J B, Park S, et al. Field monitoring of cross frames in composite steel I-girder bridges. *J. Bridge Eng*. **2024**, *29*(8): 04024049, doi:10.1061/JBENF2.BEENG-6255
12. Linzell, D.; Leon, R.T.; Zureick, A.H. Experimental and analytical studies of a horizontally curved steel I-girder bridge during erection. *J. Bridge Eng.* **2004**, *9*, 521–530, doi:10.1061/(ASCE)1084-0702(2004)9:6(521)
13. Sanchez, T.A.; White, D.W. Stability of curved steel I-girder bridges during construction. *Transp. Res. Rec.* **2012**,
14. Amani, M.; Alinia, M.M. The flexural behavior of horizontally curved steel I-girder bridge systems and single-girders. *J. Constr. Steel Res.* **2016**, *118*, 145–155, doi:10.1016/j.jcsr.2015.11.004
15. Chang, C.J.; White, D.W. An assessment of modeling strategies for composite curved steel I-girder bridges. *Eng. Struct.* **2008**, *30*, 2991–3002, doi:10.1016/j.engstruct.2008.04.011
16. Issa-El-Khoury, G.; Linzell, D.G.; Geschwindner, L.F. Computational studies of horizontally curved, longitudinally stiffened, plate girder webs in flexure. *J. Constr. Steel Res.* **2014**, *93*, 97–106, doi:10.1016/j.jcsr.2013.10.018
17. Zureick, A.; Linzell, D.; Leon, R.T.; Burrell, J. Curved steel I-girder bridges: Experimental and analytical studies. *Eng. Struct.* **2000**, *22*, 180–190, doi:10.1016/S0141-0296(98)00107-2
18. Dong, J.; Sause, R. Behavior of hollow tubular-flange girder systems for curved bridges. *J. Struct. Eng.* **2010**, *136*, 174–182, doi:10.1061/(ASCE)ST.1943-541X.0000092
19. Dong, J.; Sause, R. Finite element analysis of curved steel girders with tubular flanges. *Eng. Struct.* **2010**, *32*, 319–327, doi:10.1016/j.engstruct.2009.09.018
20. Ma, H.Y.; Sause, R. Study of horizontally curved bridge girders with tubular top flanges. *Struct. Infrastruct. Eng.* **2016**, *12*, 786–800, doi:10.1080/15732479.2015.1051998
21. Grubb, M.A.; Yadlosky, J.M.; Duwadi, S.R. Construction issues in steel curved-girder bridges. *Transp. Res. Rec.* **1996**, *1544*, 64–70, doi:10.1177/0361198196154400108
22. Transportation Research Board; National Academies of Sciences, Engineering, and Medicine. *Guidelines for Analysis Methods and Construction Engineering of Curved and Skewed Steel Girder Bridges*; The National Academies Press: Washington, DC, USA, 2012, doi:10.17226/22729

23. Ma, H.Y.; Sause, R ; M, Kourosh. Experimental and Analytical Investigation of System of Horizontally Curved Bridge Girders with Tubular Top Flanges. *Struct. Infrastruct. Eng.* **2018**, 14(12):1664-1677, doi:10.1080/15732479.2018.1486438

AUTHOR BIOGRAPHIES

	**Yuhao Li** M.E. Studying at the Department of Bridge Engineering, School of Civil Engineering, Tongji University. Research Direction: Bridge Engineering. Email: 2330857@tongji.edu.cn		**Haiying Ma** D.Eng., Associate Professor/ Doctoral Supervisor. Working at Tongji University. Research Direction: Structural Failure and Safety Performance Evaluation, New Materials and Systems, Intelligent Bridge Design and Methods. Email: mahaiying@tongji.edu.cn
	**Chivorn Sao** M.E. Studying at the Department of Bridge Engineering, School of Civil Engineering, Tongji University. Research Direction: Bridge Engineering. Email: chivorn_sao@tongji.edu.cn		**Bin Yan** D.Eng., Researcher. Working at Beijing University of Technology. Research Direction: Bridge Seismic, Widening Bridge Design, Bridge Reinforcement and Reconstruction. Email: yanbin@bjut.edu.cn
	**Qiang Liu** M.E. Graduated from Tongji University in 2023. Working at Beijing Construction Engineering Group Co., Ltd. Research Direction: Bridge Engineering. Email: 1209273553@qq.com		**Seyedmilad Komarizadehasl** D.Eng., Assistant Professor. Working at Universitat Politècnica de Catalunya (UPC) BarcelonaTech. Research Direction: Optimization of Structural Monitoring Costs, Pioneering Structural Analysis, Evaluation of Structural Pathologies. Email: milad.komary@upc.edu